Article

Cell PRESS

AMPK Is a Negative Regulator of the Warburg Effect and Suppresses Tumor Growth In Vivo

Brandon Faubert,[1,4] Gino Boily,[1,4,12] Said Izreig,[1,4,12] Takla Griss,[1,4] Bozena Samborska,[1,4] Zhifeng Dong,[4] Fanny Dupuy,[2,4] Christopher Chambers,[6] Benjamin J. Fuerth,[1,4] Benoit Viollet,[8,9,10] Orval A. Mamer,[4,5] Daina Avizonis,[4,5] Ralph J. DeBerardinis,[6,7,11] Peter M. Siegel,[2,3,4] and Russell G. Jones[1,4,*]
[1]Department of Physiology
[2]Department of Biochemistry
[3]Department of Medicine
McGill University, Montreal, QC, H3G 1Y6, Canada
[4]Goodman Cancer Research Centre
[5]Metabolomics Core Facility
McGill University, Montreal, QC H3A 1A3, Canada
[6]Children's Medical Center Research Institute
[7]McDermott Center for Human Growth and Development
University of Texas Southwestern Medical Center at Dallas, Dallas, TX 75390, USA
[8]Inserm, U1016, Institut Cochin, 75014 Paris, France
[9]CNRS, UMR 8104, 75014 Paris, France
[10]Université Paris Descartes, Sorbonne Paris Cité, 75014 Paris, France
[11]Harold C. Simmons Comprehensive Cancer Center, University of Texas Southwestern Medical Center at Dallas, Dallas, TX 75235, USA
[12]These authors contributed equally to this work
*Correspondence: russell.jones@mcgill.ca
http://dx.doi.org/10.1016/j.cmet.2012.12.001

SUMMARY

AMPK is a metabolic sensor that helps maintain cellular energy homeostasis. Despite evidence linking AMPK with tumor suppressor functions, the role of AMPK in tumorigenesis and tumor metabolism is unknown. Here we show that AMPK negatively regulates aerobic glycolysis (the Warburg effect) in cancer cells and suppresses tumor growth in vivo. Genetic ablation of the α1 catalytic subunit of AMPK accelerates Myc-induced lymphomagenesis. Inactivation of AMPKα in both transformed and nontransformed cells promotes a metabolic shift to aerobic glycolysis, increased allocation of glucose carbon into lipids, and biomass accumulation. These metabolic effects require normoxic stabilization of the hypoxia-inducible factor-1α (HIF-1α), as silencing HIF-1α reverses the shift to aerobic glycolysis and the biosynthetic and proliferative advantages conferred by reduced AMPKα signaling. Together our findings suggest that AMPK activity opposes tumor development and that its loss fosters tumor progression in part by regulating cellular metabolic pathways that support cell growth and proliferation.

INTRODUCTION

Genetic lesions that drive cancer progression affect key biological control points, including cell-cycle entry, DNA damage checkpoints, and apoptosis. However, the initiation of uncontrolled proliferation also presents a significant bioenergetic chal-

lenge to cancer cells; they must generate enough energy and acquire or synthesize biomolecules at a sufficient rate to meet the demands of proliferation. It is now appreciated that many of the predominant mutations observed in cancer also control tumor cell metabolism (Levine and Puzio-Kuter, 2010), suggesting that oncogene and tumor suppressor networks influence metabolism as part of their mode of action. One of the primary metabolic changes observed in proliferating cells is increased catabolic glucose metabolism. Many tumor cells adopt a metabolic phenotype characterized by high rates of glucose uptake and lactate production regardless of oxygen concentration, a phenomenon commonly referred to as the "Warburg effect" (Vander Heiden et al., 2009). While the energetic yield per molecule of glucose is much lower for aerobic glycolysis compared to oxidative phosphorylation (OXPHOS), the metabolic shift toward the Warburg effect appears to confer both bioenergetic and biosynthetic advantages to proliferating cells by promoting increased nonoxidative ATP production and generating metabolic intermediates from glucose that are important for cell growth (DeBerardinis et al., 2008).

Appreciation of the generality of the Warburg effect in cancer has stimulated the broader concept that a "metabolic transformation" accompanies tumorigenesis (Jones and Thompson, 2009). However, the metabolic control points and signal transduction pathways that regulate the Warburg effect during tumorigenesis and their importance to tumor progression in vivo remain poorly defined. The AMP-activated protein kinase (AMPK) is a highly conserved Ser/Thr protein kinase complex that plays a central role in the regulation of cellular energy homeostasis. AMPK is activated in response to declining fuel supply and functions in the decision to allocate nutrients toward catabolic/energy-producing or anabolic/growth-promoting metabolic pathways (Hardie, 2011). From a metabolic standpoint, AMPK promotes ATP conservation under conditions of

metabolic stress by activating pathways of catabolic metabolism such as autophagy (Egan et al., 2011; Kim et al., 2011) and inhibiting anabolic processes including lipid biosynthesis (Davies et al., 1990), TORC1-dependent protein biosynthesis (Gwinn et al., 2008; Inoki et al., 2003), and cell proliferation (Imamura et al., 2001; Jones et al., 2005). AMPK activity has been recently linked to stress resistance and survival in tumor cells (Jeon et al., 2012; Liu et al., 2012).

Due to its involvement in cellular stress resistance, AMPK has been linked to the regulation of tumorigenesis (Shackelford and Shaw, 2009). The upstream AMPK-activating kinase LKB1 is a tumor suppressor gene inactivated in patients with Peutz-Jegher's syndrome (Alessi et al., 2006), a condition that predisposes patients to gastrointestinal polyps and malignant tumors (Giardiello et al., 1987; Hearle et al., 2006). Cells lacking LKB1 display defective energy-dependent AMPK activation (Hawley et al., 2003; Shaw et al., 2004b). Additional evidence supporting a tumor suppressor function for AMPK is derived from experiments with the glucose-lowering drug metformin, which acts in part by activating AMPK (Zhou et al., 2001). Treatment of animals harboring tumor xenografts or naturally arising lymphomas with metformin can delay tumor progression (Buzzai et al., 2007; Huang et al., 2008). However, to date the role of AMPK in tumorigenesis and tumor metabolism has remained unclear.

In this work, we demonstrate that loss of AMPK signaling cooperates with Myc to accelerate tumorigenesis. Moreover, silencing AMPKα in both transformed and nontransformed cells results in a switch to aerobic glycolysis (Warburg effect) in the absence of energetic crisis. This metabolic shift is characterized by increased glucose uptake, redirection of carbon flow toward lactate, increased flux of glycolytic intermediates toward lipid biosynthesis, and an increase in net biomass (size). Induction of this metabolic shift is dependent on HIF-1α, as silencing of HIF-1α by shRNA ablates the effects of AMPKα loss on aerobic glycolysis, biosynthesis, and tumor growth in vivo. Our findings indicate that AMPK is a metabolic sensor essential for the coordination of metabolic activities that support cell growth and proliferation in cancer cells, and that disruption of AMPK signaling promotes metabolic reprogramming of cancer cells to drive the Warburg effect and influence tumor development and progression in vivo.

RESULTS

Loss of AMPKα1 Accelerates Myc-Driven Lymphomagenesis
AMPK lies downstream (Hawley et al., 2003; Shaw et al., 2004b) and upstream (Inoki et al., 2003) of known tumor suppressors (LKB1 and TSC2, respectively), but its role in tumorigenesis has remained unclear. To address this question, we generated Eμ-Myc transgenic mice (Adams et al., 1985) harboring a mutation in the gene that encodes AMPKα1 (*prkaa1*), which is the sole catalytic subunit expressed in B lymphocytes (Figure S1A available online). Latency to tumor development was monitored by palpation, and both tumor-free survival and overall life span were monitored. Compared to Eμ-Myc control mice, Eμ-Myc animals lacking AMPKα1 displayed accelerated lymphomagenesis with a median tumor onset of 7 weeks (Figure 1A) and a maximum overall survival rate of 20 weeks (Figure S1B).

Eμ-Myc mice heterozygous for AMPKα1 displayed an intermediate phenotype, with a median tumor onset of 10 weeks (Figure 1A). Lymph node tumors isolated from Eμ-Myc/α1$^{+/+}$ and Eμ-Myc/α1$^{-/-}$ mice displayed prominent B220/CD45R staining, indicating that tumors arising in these animals were of B cell origin (Figure S1C); however, all AMPKα1-deficient B220^{+} lymphomas examined lacked surface immunoglobulin (sIg) expression, suggesting that these tumors were pre-B cell tumors, rather than mature B cell tumors (Figure S1C).

To assess whether the accelerated tumor onset observed in Eμ-Myc/α1$^{-/-}$ animals was due to a cell intrinsic effect of AMPKα1 deficiency in B cells, we generated chimeric mice using Eμ-Myc/α1$^{+/+}$ or Eμ-Myc/α1$^{-/-}$ hematopoietic stem cells (HSCs) to reconstitute lethally irradiated wild-type mice (C57BL/6 background). All animals reconstituted with Eμ-Myc/α1$^{-/-}$ HSCs developed palpable lymphomas within 9 weeks of reconstitution, while only 20% of animals receiving Eμ-Myc/α1$^{+/+}$ HSCs developed tumors 12 weeks after reconstitution (Figure 1B). These data establish that specific loss of AMPKα1 in B cells can promote accelerated Myc-driven lymphomagenesis.

While lymph node tumors from both genotypes looked histologically similar by hematoxylin and eosin staining (Figure S1D), Eμ-Myc/α1$^{-/-}$ lymphomas displayed increased proliferation marker Ki-67 staining in situ (Figure 1C). Immunohistochemical (IHC) analysis revealed no major differences in tumor vascularization (measured by CD31 staining) or apoptosis (IHC for cleaved caspase-3) between AMPKα1-deficient and control Eμ-Myc tumors (Figure S1E). We next silenced AMPKα1 in primary Eμ-Myc lymphoma cells using short hairpin RNA (shRNA; Figure S1F) and measured the impact of AMPKα1 levels on cell proliferation using an in vitro competition assay. Primary Eμ-Myc lymphoma cells were transduced with retroviral vectors coexpressing GFP and control or AMPKα1-specific shRNAs, and the percentage of GFP^{+} cells remaining after 6 days of culture was determined by flow cytometry. AMPKα1 shRNA-expressing cells displayed a competitive growth advantage in vitro over cells expressing control shRNA (Figure 1D).

Activation of AMPK promotes cell survival in response to metabolic stress (Bungard et al., 2010; Buzzai et al., 2007; Jeon et al., 2012). To determine whether loss of AMPK renders Eμ-Myc tumors sensitive to metabolic stress, we treated Eμ-Myc lymphoma cells expressing control or AMPKα1 shRNAs with the glycolytic inhibitor 2-deoxyglucose (2-DG) and measured cell viability after 24 hr. AMPKα1 shRNA-expressing lymphomas displayed normal viability under standard growth conditions but increased cell death in the presence of 2-DG (Figure 1E). Together, these data suggest that loss of AMPKα1 can enhance tumor development driven by oncogenic Myc in vivo but is required to maintain tumor cell viability.

We next explored putative altered signaling events in AMPKα1-deficient lymphomas by IHC analysis of tumor sections. AMPKα, phospho-AMPKα, and phospho-ACC (pACC) expression in tumor-bearing lymph nodes confirmed a complete loss of AMPK signaling in Eμ-Myc/α1$^{-/-}$ tumors (Figure S1G). Similar to that observed in *Lkb1*$^{+/-}$ tissues (Shackelford et al., 2009; Shaw et al., 2004a), tumor tissue from Eμ-Myc/α1$^{-/-}$ mice displayed increased staining for S6 and 4E-BP1 phosphorylation (Figure 1F), suggesting an increase in basal TORC1 signaling in AMPKα-null lymphomas in vivo.
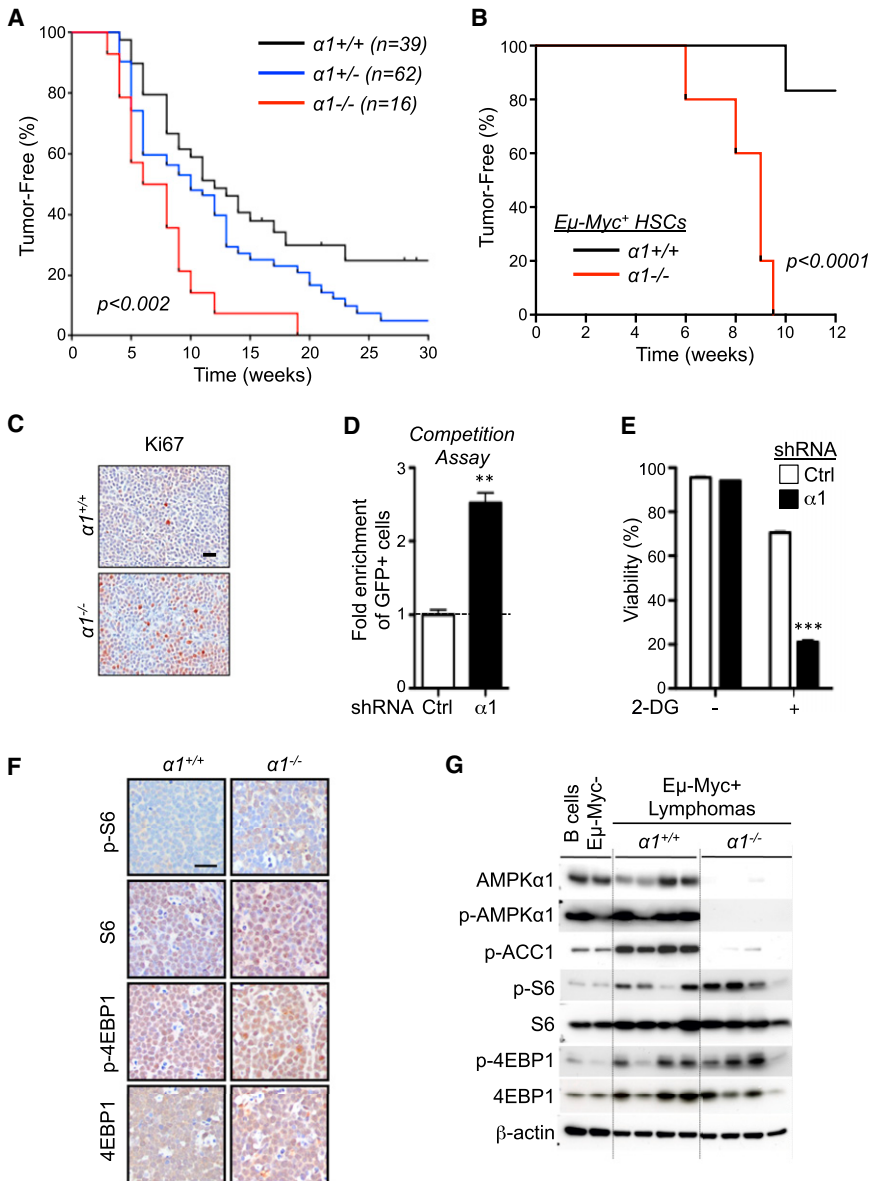
Figure 1. AMPKα1 Cooperates with Myc to Promote Lymphomagenesis

(A) Kaplan-Meier curves showing latency to tumor development in Eμ-Myc transgenic mice deficient ($α1^{-/-}$, red), heterozygous ($α1^{+/-}$, blue), or wild-type ($α1^{+/+}$, black) for AMPKα1.

(B) Kaplan-Meier curves showing latency to tumor development in chimeric mice reconstituted with Eμ-Myc/$α^{+/+}$ ($α1^{+/+}$, black) or Eμ-Myc/$α1^{-/-}$ ($α1^{-/-}$, red) HSCs (n = 5 per group).

(C) Representative histological sections of Eμ-Myc/$α^{+/+}$ and Eμ-Myc/$α1^{-/-}$ lymphomas stained for the proliferation marker Ki-67.

(D) Competition assay of Eμ-Myc lymphoma cells expressing GFP and control (Ctrl) or AMPKα1-specific (α1) shRNAs. Data are expressed as the fold enrichment in GFP+ to GFP− cells after 6 days of growth.

(E) Viability of control (Ctrl) or AMPKα1 shRNA-expressing Eμ-Myc lymphomas cells after 24 hr treatment with 2-deoxyglucose (2-DG, 15 mM). Error bars represent the SEM.

(F) Immunohistochemical analysis of representative Eμ-Myc/$α^{+/+}$ and Eμ-Myc/$α1^{-/-}$ lymphomas stained with antibodies to detect TORC1 activity (total and phospho-ribosomal S6 (pS6, S240/244), or total and phospho-4EBP1 (p4EBP1, S37/46).

(G) Immunoblot analysis of primary Eμ-Myc/$α^{+/+}$ or Eμ-Myc/$α1^{-/-}$ lymphomas. Whole-cell lysates prepared from sorted primary lymphoma cells were analyzed by immunoblot with the indicated antibodies. Each lane represents an independent tumor. Lysates from nontransformed B cells isolated from Eμ-Myc-negative mice are shown. **p < 0.01, ***p < 0.001. See also Figure S1.

lymphoma cells using nuclear magnetic resonance (NMR) spectrometry. Employing a stringent statistical cutoff (p < 0.01) and metabolites displaying a 2-fold change in abundance, we identified 13 metabolites showing differential abundance in shAMPKα1 lymphoma cells (Figure 2A). By these criteria, glucose was the only metabolite significantly decreased in shAMPKα1 lymphoma cells, while lactate displayed the greatest increase (Figure 2A). Lymphomas expressing AMPKα1 shRNA displayed an elevated extracellular acidification rate (ECAR, Figure 2B), an index of lactate production (Wu et al., 2007), but displayed no significant difference in their oxygen consumption rate (OCR; Figures 2C and S2A). AMPKα1 shRNA-expressing Eμ-Myc lymphoma cells also displayed increased glucose consumption (Figure 2D) and lactate production (Figure 2E) relative to control lymphoma cells, a metabolic signature consistent with the Warburg effect.

To assess whether reducing AMPK activity is sufficient to enhance the Warburg effect in cancer cells we silenced AMPK in two independent cell lines, H1299 (non-small-cell lung carcinoma) and HCT116 (colon carcinoma). Expression of shRNAs targeting both the α1 and α2 subunits of AMPK reduced total AMPKα protein expression in these cell lines (Figures 2F and 2G), and AMPKα silencing promoted a significant increase in
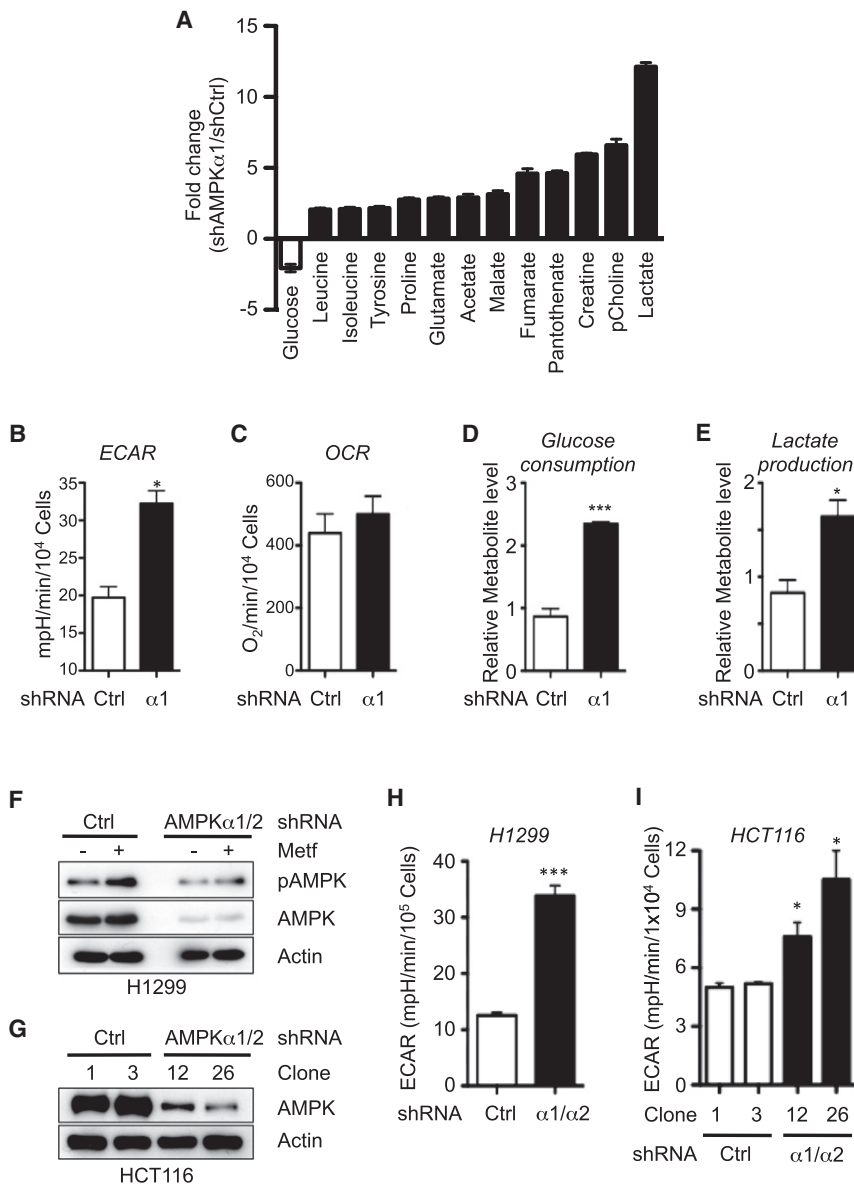
Similar data were observed via immunoblotting of primary lymphoma cells isolated immediately ex vivo from tumor-bearing lymph nodes. Both TORC1 and AMPK activity (as determined by ACC phosphorylation) were elevated in Eμ-Myc lymphoma cells compared to normal B cells (Figure 1G). When comparing Eμ-Myc/$α1^{+/+}$ and Eμ-Myc/$α1^{-/-}$ lymphomas directly, pACC levels were ablated in $α1^{-/-}$ tumors, while TORC1 activity was increased in $α1^{-/-}$ tumors with some variability in levels of both S6 and 4E-BP1 phosphorylation between $α1^{-/-}$ tumor samples (Figure 1G).

Loss of AMPKα Signaling Enhances the Warburg Effect in Cancer Cells

AMPK sits at a central node in the regulation of catabolic and anabolic metabolism (Hardie et al., 2012). To address the role of AMPK in regulating the metabolism of lymphoma cells, we conducted a targeted metabolomic analysis of Eμ-Myc

Figure 2. Loss of AMPK Signaling Enhances the Warburg Effect in Cancer Cells

(A) NMR metabolite profile of AMPKα-deficient lymphomas. Data are expressed as relative metabolite levels for shAMPKα1- versus shCtrl-expressing cells ($p < 0.01$) for samples in quintuplicate. Open bars, decreased metabolites; closed bars, increased metabolites.

(B and C) Extracellular acidification rate (ECAR) (B) and oxygen consumption rate (OCR) (C) for proliferating shControl (Ctrl) or shAMPKα1 (α1) Eμ-Myc lymphoma cells. Data represent the mean ± SEM for quadruplicate samples.

(D and E) Glucose consumption (D) and lactate production (E) of shControl (Ctrl) or shAMPKα1 (α1) Eμ-Myc lymphoma cells grown as in (B) and (C).

(F) Immunoblot of AMPKα T172 phosphorylation and total AMPKα levels in H1299 cell clones expressing control (shCtrl) or AMPKα1/α2-specific shRNAs following treatment with Metformin (5 mM, 1 hr).

(G) Knockdown of AMPKα1 and α2 in HCT116 cells.

(H and I) ECAR of H1299 (H) or HCT116 (I) cell clones expressing control (shCtrl) or AMPKα-specific (α1/α2) shRNAs grown under standard conditions.

Error bars represent the SEM. *$p < 0.05$, ***$p < 0.001$. See also Figure S2.

the basal ECAR of both H1299 (Figure 2H) and HCT116 cells (Figure 2I). Lactate production was also elevated in H1299 and HCT116 cells expressing AMPKα shRNA (Figures S2B and S2C). Taken together with our observations using AMPKα1 shRNA-expressing Eμ-Myc lymphoma cells, these data suggest that downregulation of AMPK signaling is sufficient to enhance the Warburg effect in transformed cells.

Loss of AMPK Signaling Promotes Increased ATP Levels and Anabolic Metabolism

Given the increased metabolic demands of cell proliferation, we hypothesized that an intact AMPK signaling pathway may function to coordinate metabolism and biosynthesis in actively dividing cells. To address this, we generated nontransformed mouse embryonic fibroblasts (MEFs) deficient for AMPKα. Using MEFs deficient for *prkaa1* and harboring a conditional mutation for *prkaa2* (denoted hereafter as $α1^{-/-}$, $α2^{fl/fl}$), we generated

paired isogenic cell lines that possess or completely lack AMPK catalytic activity depending on expression of Cre recombinase (Figure S3A). MEFs lacking AMPKα (Cre+) displayed increased glucose consumption (Figure S3B), lactate production (Figure S3C), and ECAR (Figure 3A) relative to control (Cre–) cells. We next traced the metabolic fate of ^{13}C-glucose in these cells, and we found that AMPKα-deficient cells displayed a progressive increase in the m+3 isotopologue of lactate (^{13}C₃-lactate) derived from glucose over time (Figure 3B), corresponding to a 6-fold increase in the glucose-to-lactate conversion rate.

One possibility for the increased ECAR in cells lacking AMPK activity could be a compensatory response to low cellular energy triggered by AMPK loss. To address this, we measured the adenylate energy charge in unstressed, actively growing MEFs by high-performance liquid chromatography (HPLC). Remarkably, cellular ATP levels were elevated in AMPKα-deficient MEFs relative to controls (Figure 3C). In contrast, the AMP:ATP ratio was not significantly affected by the loss of AMPK activity in proliferating cells (Figure 3D), suggesting no significant change in basal cellular energy charge when AMPKα is absent.

The metabolic shift to the Warburg effect facilitates the redirection of glucose-derived carbon toward biosynthetic pathways to generate biomass (Vander Heiden et al., 2009), including extrusion of glucose-derived citrate from the citric acid cycle (CAC) for lipid biosynthesis (Hatzivassiliou et al., 2005). Consistent with this, total citrate levels were elevated in AMPKα-deficient cells relative to control cells as determined by gas
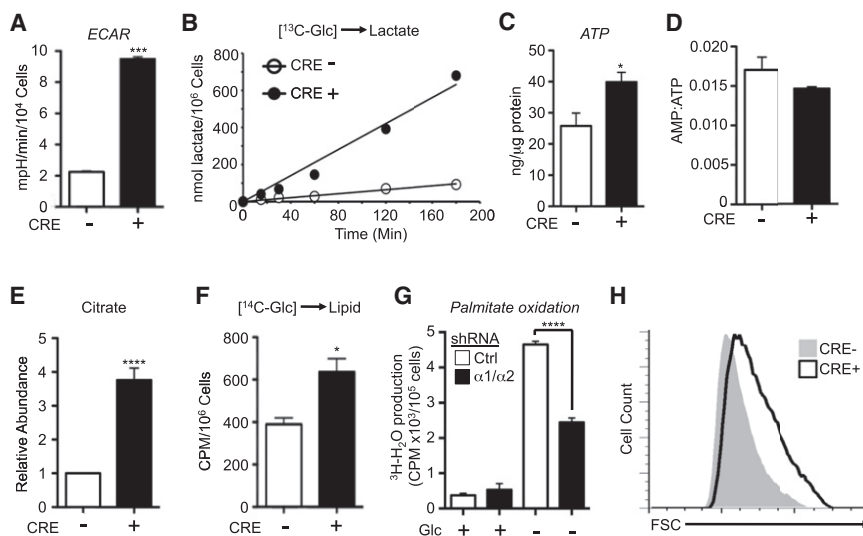
Figure 3. Loss of AMPK Signaling Promotes Increased Biosynthesis

(A) ECAR of control (Cre–, open bar) or AMPKα-null (Cre+, closed bar) MEFs cultured under standard growth conditions. Values shown are the mean ± SEM for samples in quadruplicate.

(B) Glucose-to-lactate conversion in control (Cre–) or AMPKα-deficient (Cre+) MEFs. Cells were cultured with medium containing uniformly labeled ^{13}C-glucose, and enrichment of ^{13}C-lactate (m+3) in the extracellular medium was measured at the indicated time points.

(C) ATP content of control (Cre–) or AMPKα null (Cre+) MEFs as measured by HPLC.

(D) AMP:ATP ratios for cells in (C).

(E) Intracellular citrate levels of control (Cre–) or AMPKα null (Cre+) MEFs as determined by GC-MS.

(F) Glucose-derived lipid biosynthesis in control (Cre–) or AMPKα null (Cre+) MEFs. Cells were incubated with uniformly labeled ^{14}C-glucose for 72 hr, and radioactive counts in extracted lipids were measured.

(G) Palmitate oxidation by MEFs expressing control (Ctrl) or AMPKα1/α2 shRNAs. MEFs were grown in the presence (+) or absence (–) of glucose for 24 hr, followed by culture with [9,10-^{3}H]-palmitic acid and 200 μM etomoxir. Tritiated water produced from palmitate oxidation was measured.

(H) Forward scatter (FSC) of control (Cre–, gray histogram) or AMPKα-deficient (Cre+, open histogram) MEFs.

Error bars represent the SEM. *p < 0.05, ***p < 0.001, ****p < 0.0001. See also Figure S3 and Table S1.

chromatography-mass spectrometry (GC-MS) (Figure 3E). We next measured glucose-dependent lipid biosynthesis by culturing MEFs with D-[6-^{14}C]-glucose, and we found that AMPKα-deficient cells displayed increased ^{14}C-labeling in lipids (Figure 3F). Decreased ACC phosphorylation in AMPKα-null cells is predicted to contribute to lipid synthesis, but it may also decrease fatty acid oxidation. Baseline palmitate oxidation remained low in proliferating cells grown under full glucose conditions regardless of AMPK expression (Figure 3G). However, cells expressing AMPKα shRNA displayed a reduced ability to oxidize lipid upon complete removal of glucose (Figure 3G), suggesting that AMPK is required to trigger catabolic lipid metabolism specifically under nutrient poor conditions.

Consistent with shunting of glucose-derived carbon toward biosynthesis in proliferating cells, AMPKα-null MEFs displayed a 20% increase in median cell size as determined by forward scatter (FSC) with flow cytometry (Figure 3H). TORC1 is a central regulator of cell size (Laplante and Sabatini, 2009), and AMPK can negatively regulate TORC1 activity under energy stress (Inoki et al., 2003; Shaw et al., 2004a). Consistent with this, the AMPK agonist AICAR suppressed TORC1 activity (as determined by reduced pS6 and p4E-BP levels) only in cells with wild-type AMPKα (Figure S3D). Notably, growth factor-dependent TORC1 activity in cells was similar regardless of AMPKα status (Figure S3E), suggesting the existence of TORC1-independent pathways of biomass regulation in AMPKα-deficient cells.
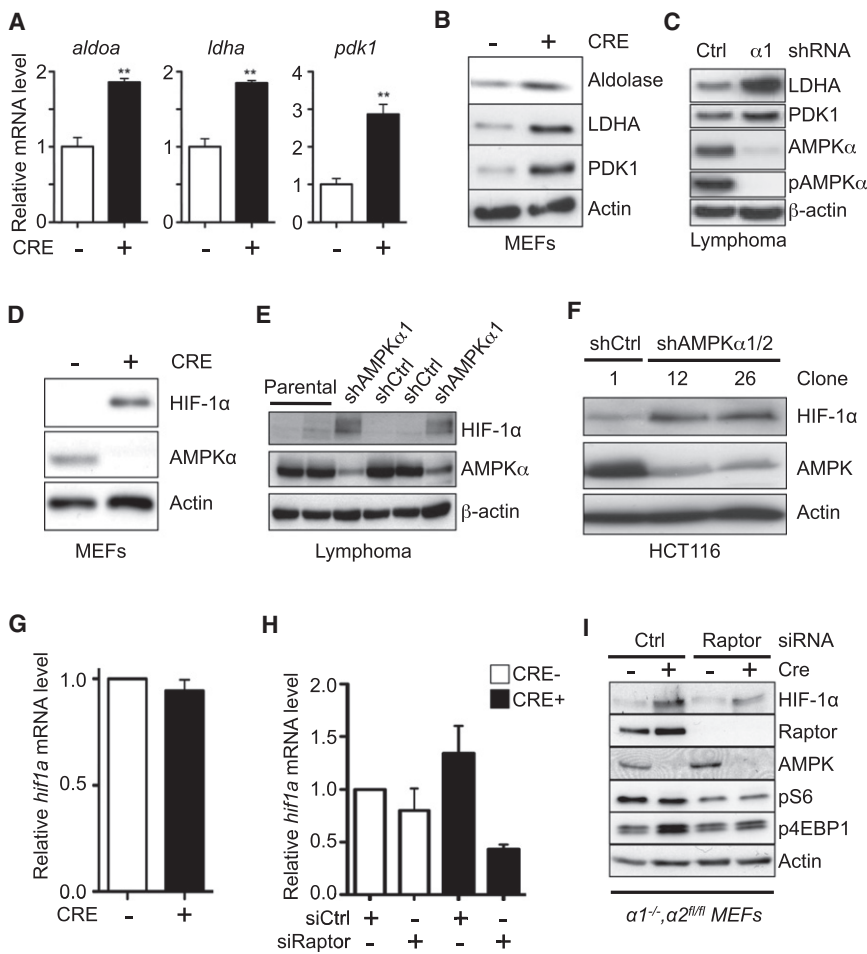
Loss of AMPKα Promotes a Glycolytic Signature and Increased HIF-1α Expression

We next investigated potential mechanisms governing the glycolytic phenotype associated with AMPKα-deficient cells. We first used quantitative PCR (qPCR) to examine the relative levels of messenger RNA (mRNA) transcripts encoding for proteins involved in glycolytic regulation. AMPKα-null MEFs displayed a

glycolytic gene signature marked by increased mRNA expression of Aldolase A (*aldoa*), Lactate dehydrogenase A (*ldha*), and pyruvate dehydrogenase kinase 1 (*pdk1*) (Figures 4A and S4A), a pattern of gene expression also displayed by shAMPKα1 lymphoma cells (Figure S4B). Elevated Aldolase, LDHA, and PDK1 protein levels were also detected in AMPKα-deficient MEFs (Figure 4B) and shAMPKα1 lymphoma cells (Figure 4C).

PDK1 curbs pyruvate flux to Acetyl-CoA and entry into the TCA cycle by antagonizing the action of the pyruvate dehydrogenase (PDH) complex (Kim et al., 2006; Papandreou et al., 2006). Thus, elevated PDK1 levels observed in AMPKα-deficient cells may be predicted to affect glucose flux to citrate. To measure this, we cultured control or AMPKα-null MEFs in medium containing uniformly labeled [^{13}C]-glucose and measured ^{13}C enrichment in citrate by gas chromatography-mass spectrometry (GC-MS). Glucose-derived pyruvate is converted to Ac-CoA by PDH. Subsequent condensation of [1,2-^{13}C]-Ac-CoA with oxaloacetate (OAA) yields citrate with 2 additional mass units (m+2), while an additional turn through the TCA cycle produces citrate(m+4). We observed modest increases in levels of unlabeled citrate in AMPKα null MEFs relative to control cells, as well as reduced citrate(m+4) labeling from [^{13}C]-glucose (Figure S4C). ^{13}C enrichment in citrate was similar between control and AMPKα-null MEFs when [^{13}C]-glutamine was used as carbon source (Figure S4D).

Several of the enzymes elevated in AMPKα-deficient cells are known targets of the transcription factor HIF-1α, one of the central regulators of glycolysis induced by hypoxia (Keith et al., 2012; Semenza, 2011). We observed elevated HIF-1α protein levels under normoxia after acute AMPKα deletion in our isogenic cell lines (Figure 4D), consistent with previous work demonstrating elevated HIF-1α protein expression in cells with chronic depletion of AMPKα (Shackelford et al., 2009). Moreover, shRNA-mediated knockdown of AMPKα1 in Eμ-Myc

Figure 4. Loss of AMPK Promotes a Glyco-lytic Signature and Increased HIF-1α Expression

(A) Relative expression of *aldoa*, *ldha*, and *pdk1* mRNA in control (Cre–, open bar) or AMPKα-null (Cre+, closed bar) MEFs as determined by qPCR. Transcript levels were determined relative to *actin* mRNA levels and normalized relative to control (Cre–) cells.

(B and C) Immunoblot analysis of Aldolase, LDHA, and PDK1 protein levels in whole-cell lysates from control (Cre–) and AMPKα-null (Cre+) MEFs (B) or shControl (Ctrl) and shAMPKα1 (α1) -expressing Eμ-Myc lymphoma cells (C).

(D and F) Immunoblot of HIF-1α protein levels in whole-cell lysates from control (Cre–) and AMPKα-null (Cre+) MEFs (D), shControl (shCtrl) and shAMPKα1-expressing Eμ-Myc lymphoma cells (E), or HCT116 cell clones expressing control (shCtrl) or AMPKα-specific (shAMPKα1/2) shRNAs (F). All cells were grown under 20% O_2.

(G) Relative *hif1a* mRNA expression in control (Cre–) or AMPKα null (Cre+) MEFs as determined by qPCR.

(H and I) Expression of *hif-1α* mRNA (H) and protein levels (I) for control (Cre–) or AMPKα null (Cre+) MEFs transfected with siRNAs targeting Raptor. Protein lysates were also analyzed for pS6 and p4EBP levels by immunoblot. Raptor, AMPKα, and actin levels are shown as controls.

Error bars represent the SEM. **p < 0.01. See also Figure S4.

lymphomas (Figure 4E) or HCT116 cells (Figure 4F) promoted normoxic HIF-1α protein stabilization. Levels of *hif1a* mRNA were unchanged in AMPKα null MEFs relative to controls (Figure 4G), suggesting that reduction of AMPK activity is sufficient to increase HIF-1α protein levels in cancer cells under normoxic conditions independent of mRNA levels.

TORC1 signaling has been linked to control of HIF-1α expression through differential regulation of its translation (Choo et al., 2008). To examine the contribution of TORC1 signaling to HIF-1α stabilization in AMPKα-deficient cells, we silenced the TORC1 binding partner Raptor using small interfering RNA (siRNA). Treatment with Raptor siRNA significantly reduced *hif1a* mRNA levels in both control and AMPKα-deficient MEFs, with the latter demonstrating a large drop in *hif1a* mRNA expression upon Raptor depletion (Figure 4H). Moreover, transient knockdown of Raptor in AMPKα-deficient MEFs reduced HIF-1α protein levels (Figure 4I) and reduced the expression of the HIF-1α targets *aldoa* (Figure S4E) and *ldha* (Figure S4F).

## AMPKα-Dependent Effects on Glycolysis Are Mediated by HIF-1α

To determine the contribution of HIF-1α to the glycolytic phenotype observed in AMPKα null cells, we stably silenced HIF-1α in control (Cre–) or AMPKα-deficient (Cre+) MEFs using RNA interference. Expression of HIF-1α shRNA ablated HIF-1α protein

expression in AMPKα-deficient MEFs under normoxia (Figure 5A) and blocked CoCl$_2$-dependent induction of HIF-1α protein in both AMPKα-deficient and control cells (Figure S5A). Expression of HIF-1α shRNA reduced *pdk1* mRNA in AMPKα-null cells to control levels, demonstrating that expression of this shRNA could block HIF-1α-dependent transcription (Figure 5B). We next determined whether silencing HIF-1α could reverse the Warburg effect triggered by loss of AMPKα activity. While HIF-1α shRNA had little effect on the ECAR of control cells, silencing HIF-1α in AMPKα-deficient cells lowered the ECAR below control levels (Figure 5C). GC-MS analysis revealed dramatic reductions in intracellular pyruvate and lactate in AMPKα-deficient cells expressing HIF-1α shRNA relative to control shRNA (Figure 5D). Moreover, silencing of HIF-1α ablated the enhanced levels of glucose consumption (Figure 5E) and lactate production (Figure 5F) displayed by AMPKα-deficient cells. Similar reductions in glucose consumption and lactate production were observed in AMPKα-deficient MEFs transfected with HIF-1α siRNA (Figures S5B–S5D). Silencing of Raptor in AMPKα-deficient MEFs, which partially reduced HIF-1α protein levels (Figure 4I), led to slight reductions in lactate production (Figure S5E) and ECAR (Figure S5F).

HIF-1α Drives Increased Biosynthesis in AMPKα-Null Cells

Next we determined the impact of HIF-1α expression on cellular biosynthesis and proliferation induced by AMPKα loss. Silencing
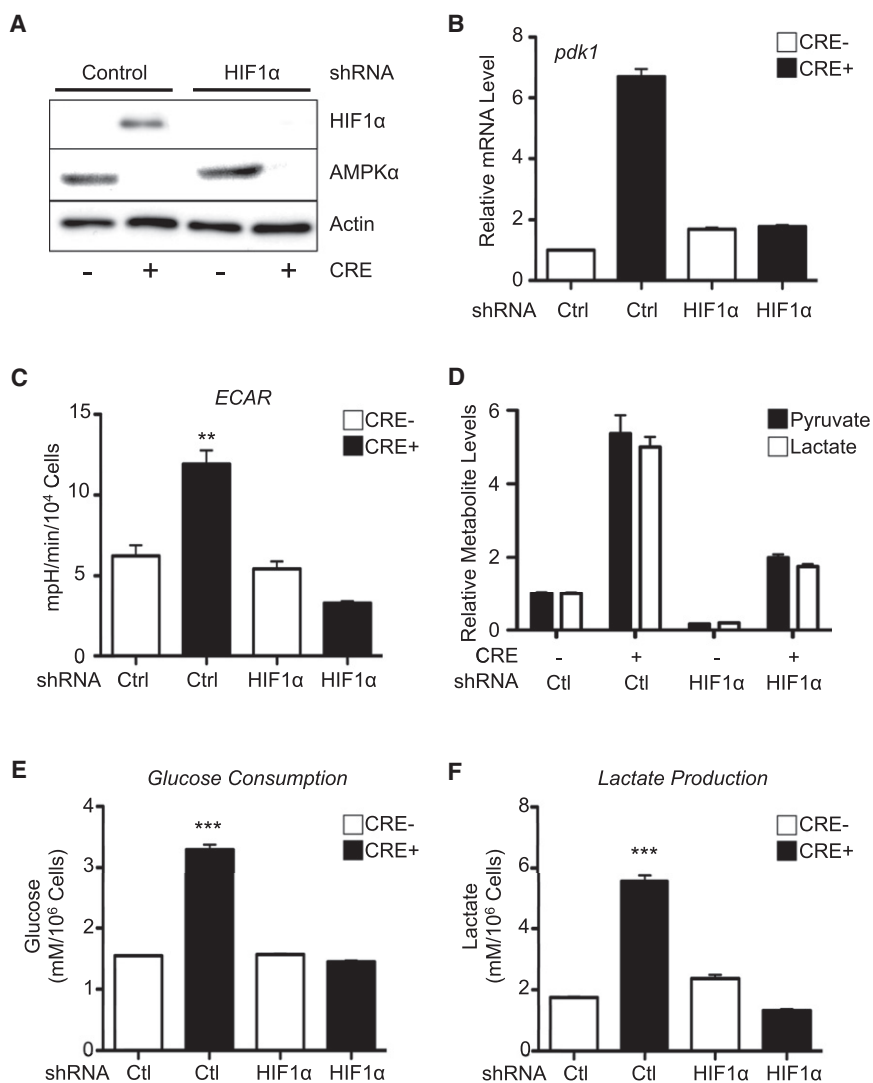
Figure 5. HIF-1α Mediates the Effects of AMPK Loss on Aerobic Glycolysis

(A) HIF-1α protein expression in control (Cre–) or AMPKα-deficient (Cre+) MEFs also expressing control or HIF-1α-specific shRNAs. Cells were grown under normoxic conditions (20% O_2). AMPKα and actin protein levels are shown.

(B) Relative expression of *pdk1* mRNA in control (Cre–) or AMPKα-deficient (Cre+) MEFs expressing control (Ctrl) or HIF-1α-specific shRNAs.

(C–F) AMPK-dependent changes in the Warburg Effect are dependent on HIF-1α.

(C) ECAR of control (Cre–) or AMPKα-deficient (Cre+) MEFs expressing control (Ctrl) or HIF-1α-specific shRNAs grown under normoxic conditions (20% O_2).

(D–F) Relative intracellular pyruvate (closed bars) and lactate (open bars) levels (D), glucose consumption (E), and lactate production (F) for cells grown as in (C).

Error bars represent the SEM. **p < 0.01, ***p < 0.001. See also Figure S5.

AMPKα-deficient cells reduced their overall rate of proliferation (Figure 6D). Collectively, the data suggest that AMPK negatively regulates the metabolic (Warburg effect) and biosynthetic programs of proliferating cells through the inhibition of HIF-1α function.

## HIF-1α Is Required for the Progression of AMPKα1-Deficient Lymphomas

Our earlier results (Figure 2) indicate that reduced AMPK signaling synergizes with Myc to promote the Warburg effect in lymphoma. To determine the contribution of HIF-1α to the glycolytic phenotype of Eμ-Myc lymphoma cells, we stably expressed HIF-1α-specific shRNAs in Eμ-Myc lymphoma cells with silenced AMPKα1. Silencing of HIF-1α in AMPKα1 shRNA-expressing cells reduced HIF-1α protein expression to control levels (Figure 7A). Protein levels of the HIF-1α targets Aldolase and LDHA expression also decreased when HIF-1α was silenced in AMPKα1 shRNA-expressing lymphomas (Figure 7A). We next examined metabolic activity in these lymphomas. Expression of AMPKα1 shRNA increased cellular ECAR as expected, while silencing of HIF-1α reduced this enhanced ECAR response by 60% (Figure 7B). Finally, lymphoma cells expressing both AMPKα1 and HIF-1α shRNA showed decreased proliferation relative to cells expressing AMPKα1 shRNA alone (Figure 7C).

We next tested the requirement for HIF-1α for tumor progression in vivo. Primary control or AMPKα-deficient Eμ-Myc lymphoma cells were transduced with retroviral vectors expressing GFP and either control or HIF-1α shRNAs, and the percentage of GFP+ lymphoma cells (expressing the shRNA of interest) was determined by flow cytometry prior to transplantation into recipient mice and after lymphoma formation

of HIF-1α reduced intracellular citrate in AMPKα-deficient cells by approximately 70% (Figure 6A), restoring citrate levels to that observed in control cells. Moreover, suppression of HIF-1α dramatically reduced glucose-dependent lipogenesis in AMPKα-deficient MEFs (Figure 6B). Suppression of HIF-1α had little effect on glucose-dependent lipogenesis in control cells (Figure 6B), consistent with the fact that HIF-1α protein is maintained at low levels in these cells under normoxia.

Given that aberrant HIF-1α expression drives both enhanced glycolysis and glucose-derived lipogenesis, we reasoned that the increased size of AMPKα-deficient cells may be attributed to HIF-1α-dependent changes in anabolic metabolism. While loss of AMPKα promotes increased cell size, silencing of HIF-1α restored the size of AMPKα-deficient MEFs to that of control cells (Figure 6C). Notably, rapamycin treatment also reduced the size of AMPKα-deficient MEFs (Figure S6A). However, this treatment also reduced *hif1a* mRNA levels in cells regardless of AMPKα expression (Figure S6B), suggesting that rapamycin may exert its effects in part through regulation of HIF-1α mRNA. Finally, suppression of HIF-1α signaling in
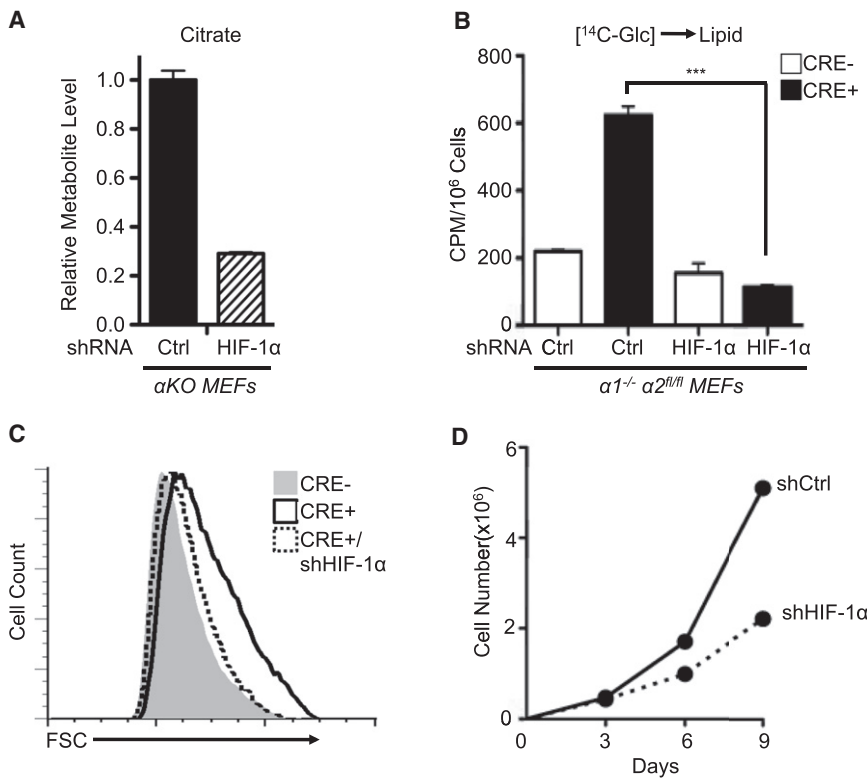
Figure 6. HIF-1α Drives Increased Biosynthesis and Proliferation of AMPKα-Null Cells

(A) Relative citrate abundance in metabolite extracts from AMPKα-deficient (αKO) MEFs expressing control (Ctrl) or HIF-1α-specific shRNAs as determined by GC-MS.

(B) Lipid biosynthesis in AMPKα-deficient MEFs with HIF-1α knockdown. Control (Cre–) or AMPKα-deficient (Cre+) MEFs expressing control (Ctrl) or HIF-1α-specific shRNAs were incubated with uniformly labeled ^{14}C-glucose for 72 hr, and radioactive counts in extracted lipids were measured.

(C) Cell size of control (gray histogram), AMPKα-null (open histogram), and AMPKα-null MEFs expressing HIF-1α shRNA (dashed histogram) as measured by FSC intensity.

(D) Growth curves of AMPKα-null MEFs expressing control (shCtrl) or HIF-1α-specific (shHIF-1α) shRNAs grown under 20% O$_2$. Growth curves were determined using a 3T3 growth protocol and cell counts measured by trypan blue exclusion.

Error bars represent the SEM. ***p < 0.001. See also Figure S6.

(Figure 7D). Expression of control shRNA did not dramatically alter the fraction of GFP$^+$ Eμ-Myc lymphoma cells regardless of genotype (Figures 7E and 7F). Interestingly, silencing of HIF-1α in Eμ-Myc lymphomas promoted a general increase in the number of GFP$^+$ tumor cells, although this did not reach statistical significance (Figure 7F). However, lymphoma cells expressing HIF-1α shRNA were selectively depleted in AMPKα-null tumors (Figures 7E and 7F). Collectively, these data suggest that loss of AMPK signaling promotes a metabolic and growth advantage in lymphoma cells and that HIF-1α is required for the growth of AMPKα1 null tumors in vivo.

DISCUSSION

AMPK is a cellular energy sensor that coordinates metabolic activities in many tissues. Under conditions of energetic stress, AMPK activation suppresses cell growth and proliferation, leading to speculation that AMPK may function as part of a tumor suppressor pathway (Hardie, 2011; Shackelford and Shaw, 2009). Here we provide genetic evidence that AMPKα displays tumor suppressor activity in vivo. Loss of AMPK signaling cooperates with oncogenic Myc to enhance tumorigenesis in a mouse model of lymphomagenesis, suggesting that AMPK may function as a tumor suppressor (Figure 1). Moreover, we demonstrate that AMPK is a negative regulator of both aerobic glycolysis and cellular biosynthesis in cancer cells. Cells deficient for the catalytic alpha subunit(s) of AMPK display increased aerobic glycolysis marked by increased lactate production from glucose (Figures 2 and 3), and downregulation of AMPK activity is sufficient to induce the Warburg Effect in cancer cells (Figure 2). We find that HIF-1α is a key mediator of AMPK-dependent

effects on cellular metabolism. Reduction of AMPKα levels in cells leads to increased HIF-1α protein levels under normoxia in both transformed and non-transformed cells (Figure 4), and HIF-1α is required to drive both the Warburg effect and the growth of AMPKα1-deficient lymphomas in vivo (Figure 5, 6, and 7). The results presented here suggest that the downregulation of AMPK activity eliminates a key metabolic checkpoint that normally antagonizes anabolic progrowth cellular metabolism. Thus, AMPK may act in cancer cells as a metabolic gatekeeper that functions to establish metabolic checkpoints that limit cell division, and its loss of function can enhance both tumorigenesis and tumor progression.

All cells must manage their energetic resources to survive. We and others have established that AMPK is the central mediator of a metabolic cell-cycle checkpoint activated in response to nutrient limitation in mammalian cells (Gwinn et al., 2008; Inoki et al., 2003; Jones et al., 2005). However, programs of ATP production and macromolecular synthesis must also be coordinated in proliferating cells to ensure proper cell division. The data presented here suggest that AMPK functions to regulate metabolic homeostasis in proliferating cells in the absence of acute energetic stress. Isogenic MEFs or cancer cells lacking AMPKα activity display a metabolic shift toward aerobic glycolysis, thus allowing cancer cells to engage aerobic glycolysis for ATP production and divert glucose-derived CAC intermediates toward lipid biosynthesis to support increased cell growth. AMPK may also influence lipid biosynthesis through regulation of ACC and other lipogenic enzymes, possibly through its effects on SREBP-1 (Li et al., 2011). Thus, defective AMPKα signaling promotes the rewiring of metabolic pathways to favor cell growth pathways.

Interestingly our data provide evidence that AMPKα-deficient tumors display increased activation of the TORC1 targets S6 and
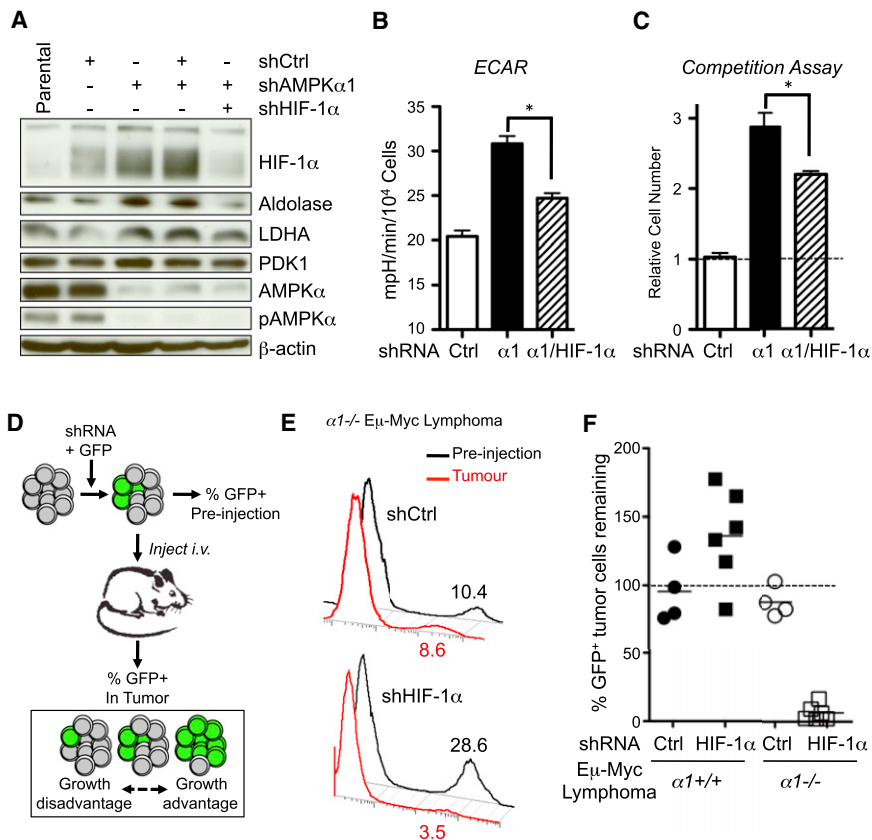
Figure 7. HIF-1α Mediates the Metabolic and Tumorigenic Effects Induced by AMPKα1 Loss
(A) Immunoblots of whole-cell lysates from Eμ-Myc lymphoma cells expressing AMPKα1 and HIF-1α shRNAs. Cells were cultured under standard conditions (25 mM glucose, 20% O_2). Blots were probed with antibodies to the indicated proteins.
(B) ECAR of Eμ-Myc lymphoma cells expressing control (Ctrl), AMPKα1 (α1), or both AMPKα1 and HIF-1α (α1/HIF-1α) shRNAs and grown under standard conditions.
(C) Competition assay of Eμ-Myc lymphoma cells infected with retrovirus expressing GFP and control, AMPKα1 (α1), or both AMPKα1 and HIF-1α (α1/HIF-1α) shRNAs. The data are expressed as the relative increase in GFP^+ to GFP^- cells after 6 days of culture.
(D) Schematic of in vivo lymphoma competition assay.
(E) Representative histograms of GFP expression for $AMPKα1^{-/-}$ Eμ-Myc lymphoma cells prior to injection into recipient mice (preinjection, black) or isolated from lymph node tumors (tumor, red). Numbers indicate the percentage of GFP^+ cells.
(F) Percent recovery of GFP^+ tumor cells from individual Eμ-Myc/α1^{+/+} (black) or Eμ-Myc/α1^{−/−} (white) tumors expressing the indicated shRNAs. Error bars represent the SEM. *p < 0.05.

4E-BP1, suggesting that AMPK, as opposed to other AMPK-related kinases, may be the key TORC1 regulator downstream of LKB1 in tumors. Consistent with past work (Inoki et al., 2003; Liu et al., 2006; Shaw et al., 2004a), we find that AMPK functions to downregulate TORC1 activity specifically under conditions of energetic stress, when it is desirable to suppress ATP-consuming processes such as mRNA translation. This may provide a metabolic advantage to proliferating cells, where the loss of AMPK signaling promotes increased ATP production and resource accumulation without affecting the mitogenic properties of TORC1. By concurrently silencing AMPK while maintaining TORC1 signaling, cells may effectively bypass endogenous brakes on cellular metabolism, supporting increased tumor cell growth and proliferation.

Our work here establishes HIF-1α as a key mediator of the metabolic transformation triggered by reduced AMPKα activity in cancer cells. We show that downregulation of AMPK signaling is sufficient to induce normoxic HIF-1α stabilization and enhance the Warburg effect. TORC1 activity appears to contribute in part to this process, as silencing of the mTORC1 binding partner Raptor reduces levels of *hif1a* mRNA in AMPKα-deficient cells. However, silencing of Raptor moderately reduces HIF-1α protein levels and has a minimal effect on the glycolytic phenotype of AMPKα-deficient cells, suggesting that AMPK may regulate HIF-1α-dependent Warburg metabolism through additional mechanisms. Interestingly, TORC1 inhibition reduces *hif1a* mRNA and reduces glycolysis in cells regardless of AMPK expression, suggesting that TORC1 may function on a more

global level as a positive regulator of glycolysis beyond specific effects on HIF-1α expression (Düvel et al., 2010). Given that TORC1 signaling is elevated in AMPKα1-deficient lymphomas, this may have implications for tumor metabolism in vivo. HIF-1α mRNA levels are unaffected by AMPK expression; thus, AMPK may affect normoxic HIF-1α protein expression either through decreased protein turnover or differential translation of HIF-1α mRNA (Choo et al., 2008). Overall, we propose that AMPK functions to coordinate glycolytic and oxidative metabolism in proliferating cells by restricting HIF-1α function.

One consequence of AMPK loss in cells is enhanced flux of glucose-derived carbon to citrate for lipid biosynthesis, promoting biomass accumulation and increased cell size. This may appear to be counterintuitive, as HIF-1α-dependent upregulation of PDK1 under hypoxia is proposed to direct glucose-derived carbon away from the CAC (Kim et al., 2006; Papandreou et al., 2006). However, glucose-to-citrate flux is not blocked in AMPKα-null cells, despite elevated PDK1 levels. Rather, the reduced levels of citrate(m+4) in AMPKα-null cells may result from increased use of glucose-derived citrate(m+2) for lipid biosynthesis. Reduction of AMPK levels significantly decreases ACC1 inhibition in both tumor cells and tumor tissue, which would permit maximal activity of ACC1 for lipid biosynthesis. Thus, AMPK may regulate lipid biosynthesis and biomass accumulation on multiple levels: substrate availability (HIF-1α-dependent glucose-derived citrate) and ACC activity.

We propose that AMPK may function as a metabolic tumor suppressor, limiting the growth of cancer cells by regulating

key bioenergetic and biosynthetic pathways required to support unchecked proliferation. Thus, selection against AMPK activity may represent an important regulatory step for tumor initiation and progression, allowing tumor cells to gain a metabolic growth advantage. Reduced AMPK activity has been detected in primary human breast cancer (Hadad et al., 2009), and reduced expression of *prkaa2*, the gene that encodes for AMPKα2, has been linked to human breast, ovarian, and gastric cancer (Hallstrom et al., 2008; Kim et al., 2012). It is also well documented that LKB1 deficiency (Shackelford and Shaw, 2009) or genetic events that target LKB1 activity (Godlewski et al., 2010; Zheng et al., 2009) lead to reduced AMPK signaling in tumor cells. Thus, there may be several routes by which AMPK function is suppressed in tumors to provide a selective metabolic growth advantage.

While selection for loss of AMPK function may favor the Warburg effect in tumor cells, it may also eliminate metabolic checkpoints essential for cellular adaptation to stress. AMPK normally plays a protective role to block cell growth in response to poor nutrient conditions, and as such its loss or suppression during tumorigenesis may sensitize tumor cells to apoptosis under hypoxic or nutrient depleted environments (Svensson and Shaw, 2012). Consistent with this, silencing AMPKα1 in Eμ-Myc lymphomas conferred sensitivity to apoptosis induced by the glycolytic inhibitor 2-DG. The increased levels of ACC phosphorylation observed in Eμ-Myc tumors (Figure 1) imply that lymphomas experience metabolic stress and AMPK activation in vivo. Thus, while ablation of AMPK signaling may enhance tumorigenesis, inhibition of this central energy-sensing pathway may offer unique a therapeutic window for the treatment of tumors with metabolic inhibitors. Our data provide a mechanistic rationale in support of the use of AMPK agonists such as metformin for cancer therapy (Buzzai et al., 2007; Evans et al., 2005), as the efficacy of these agents against tumor growth may lie in their ability to engage AMPK-dependent metabolic checkpoints to restrict anabolic growth. Understanding the reprogramming of cellular metabolic networks by AMPK in cancer may aid in the development of novel approaches for cancer therapy.

EXPERIMENTAL PROCEDURES

Cell Lines, DNA Constructs, and Cell Culture

Primary MEFs deficient for *prkaa1* ($\alpha 1^{-/-}$) and conditional for *prkaa2* ($\alpha 2^{fl/fl}$) were generated by timed mating as previously described (Jones et al., 2005) and immortalized with SV40 Large T Antigen. HCT116 cells were obtained from ATCC. Primary Eμ-Myc lymphoma cells were provided by Jerry Pelletier (Robert et al., 2009). DNA plasmids MiCD8t, pKD-HIF-1α hp, and LMP-based shRNAs against mouse and human AMPKα1 and α2 have been described previously (Bungard et al., 2010; Jones et al., 2005; Lum et al., 2007). AMPKα-deficient MEFs were generated by transduction of $\alpha 1^{-/-}$, $\alpha 2^{fl/fl}$ MEFs with Cre-expressing retrovirus to delete α2-floxed alleles. For siRNA transfections, cells were subjected to two rounds of reverse transfection with pooled siRNAs against HIF-1α (Dharmacon) with Lipofectamine RNAimax (Hatzivassiliou et al., 2005). AMPK activity was assessed in cell lines after stimulation with AICAR (1 mM, Toronto Research Chemicals) or metformin (5 mM, Sigma) for 1 hr. For induction of HIF-1α protein expression, cells were treated with $CoCl_2$ (100 μM) for 1 hr. For mass isotopomer analysis, cells were incubated in glucose- or glutamine-free medium containing 10% dialyzed FBS and uniformly labeled [^{13}C]-glucose or [^{13}C]-glutamine, respectively (Cambridge Isotope Laboratories).

Mice

Mice deficient for AMPKα1 (Mayer et al., 2008), floxed for AMPKα2 (Jørgensen et al., 2004), and Eμ-Myc transgenic mice (Adams et al., 1985) have been

described previously. Eμ-Myc/$\alpha 1^{-/-}$ mice (and littermate controls) were generated by breeding of AMPKα1-deficient and Eμ-Myc transgenic mouse strains. Mice were bred and maintained under specific pathogen-free conditions at McGill University under approved protocols.

Determination of Cell Proliferation, Competition Assays, and Cell Size

Cell proliferation curves for all cell lines was determined by cell counting with trypan blue exclusion and a TC10 Automated Cell Counter (BioRad). For in vitro competition assays, primary Eμ-Myc lymphoma cells were transduced with retroviral vectors coexpressing GFP and AMPKα1-specific shRNA or control shRNA, and the percentage of GFP-positive cells remaining after 6 days of culture was determined by flow cytometry. Cell size of viable cells was quantified as the mean fluorescence intensity for FSC with flow cytometry. All flow cytometry was conducted with BD FACSCalibur (BD Biosciences) or Gallios (Beckman Coulter) flow cytometers and analyzed with FlowJo software (Tree Star).

Immunoblotting

Cells were lysed in modified CHAPS buffer (10 mM Tris-HCl, 1 mM $MgCl_2$, 1 mM EGTA, 0.5 mM CHAPS, 10% glycerol, and 5 mM NaF) or AMPK lysis buffer (MacIver et al., 2011) supplemented with protease and phosphatase inhibitors (Roche), DTT (1 μg/ml), and benzamidine (1 μg/ml). Cleared lysates were resolved by SDS-PAGE, transferred to nitrocellulose, and incubated with primary antibodies. Primary antibodies to AMPK (pT172-specific and total), AMPKα2, ACC (pS79 and total), p70 S6 kinase (pT389-specific and total), S6 ribosomal protein (pS235/236-specific and total), 4E-BP1 (pT37/46-specific and total), LDHA, PDK1, Aldolase, and actin were obtained from Cell Signaling Technology. Anti-HIF-1α antibodies were from Cayman Biomedical.

Quantitative Real-Time PCR

Total mRNA was isolated from cells with Trizol, and complementary DNA (cDNA) was synthesized from 100 ng total RNA with the Superscript VILO cDNA Synthesis Kit (Invitrogen). Quantitative PCR was performed with SYBR Green qPCR SuperMix (Invitrogen) and an Mx3005 qPCR machine (Agilent Technologies) with primers against *aldoA*, *ldha*, *pdk1*, *hif1a*, and *actin*. All samples were normalized to β-actin mRNA levels. Primer sequences are listed in Table S1.

Metabolic Assays

Respirometry (OCR) and the extracellular acidification rate (ECAR) of cells were measured with an XF24 Extracellular Flux Analyzer (Seahorse Bioscience). In brief, cells were plated at 5×10^4/well in 625 μl nonbuffered Dulbecco's modified Eagle's medium containing 25 mM glucose and 2 mM glutamine. Cells were incubated in a CO_2-free incubator at 37°C for 1 hr to allow for temperature and pH equilibration prior to loading into the XF24 apparatus. XF assays consisted of sequential mix (3 min), pause (3 min), and measurement (5 min) cycles, allowing for determination of OCR/ECAR every 10 min.

Glucose consumption and lactate production were determined via enzymatic assays described previously (Buzzai et al., 2007). Glucose-derived lipid biosynthesis was determined by culturing of cells in medium containing ^{14}C-glucose for 3 days, and extracted lipids with a 1:1:1 Water/Methanol/Chloroform extraction procedure (Mullen et al., 2012). After extraction, the organic layer was isolated, dried via N_2 stream, resuspended in methanol, and incorporated radioactivity measured with a MicroBeta Liquid Scintillation Counter (Perkin Elmer).

Analysis of Metabolites by NMR and GC-MS

Metabolites from tissue culture cells were extracted as described previously (Xu et al., 2011). In brief, cells ($2–5 \times 10^6$/10 cm dish) were washed three times with ice-cold 0.9% saline solution. Cells were lysed with ice-cold 80% methanol followed by sonication (Diagenode Bioruptor), and extracts were dried by vacuum centrifugation. For NMR analysis, cell extracts were resuspended in 220 ml ^2H_2O containing 0.2 mM 4,4-dimethyl-4-silapentane-1-sulfonic acid (DSS), 0.1 mM difluorotrimethylsilanylphosphonic acid (DFTMP), and 0.01 mM sodium azide. NMR data collection was performed at the Québec/Eastern

Canada High Field NMR Facility on a 500 MHz Inova NMR system (Agilent Technologies) equipped with an HCN cryogenically cooled probe operating at 25 K. Metabolite chemical shift assignments were confirmed by total correlation spectroscopy, and targeted metabolites were profiled with a 500 MHz metabolite library from Chenomx.

For GC-MS analysis, dried samples were resuspended in 30 μl anhydrous pyridine and added to GC-MS autoinjector vials containing 70 μl N-(tert-butyl-dimethylsilyl)-N-methyltrifluoroacetamide (MTBSTFA) derivatization reagent. The samples were incubated at 70°C for 1 hr, after which aliquots of 1 μl were injected for analysis. GC-MS data were collected on an Agilent 5975C series GC/MSD system (Agilent Technologies) operating in election ionization mode (70 eV) and selected ion monitoring. Quantified metabolites were normalized relative to protein content (μg).

Statistical Analysis

Statistics were determined with a paired Student's t test, ANOVA, or log-rank (Mantel-Cox) test with Prism software (GraphPad). Data are calculated as the mean ± SEM unless otherwise indicated. Statistical significance is represented in figures by $*p < 0.05$, $**p < 0.01$, $***p < 0.001$, and $****p < 0.0001$.

SUPPLEMENTAL INFORMATION

Supplemental Information includes six figures and one table and can be found with this article online at http://dx.doi.org/10.1016/j.cmet.2012.12.001.

REFERENCES

Adams, J.M., Harris, A.W., Pinkert, C.A., Corcoran, L.M., Alexander, W.S., Cory, S., Palmiter, R.D., and Brinster, R.L. (1985). The c-myc oncogene driven by immunoglobulin enhancers induces lymphoid malignancy in transgenic mice. Nature 318, 533–538.

Alessi, D.R., Sakamoto, K., and Bayascas, J.R. (2006). LKB1-dependent signaling pathways. Annu. Rev. Biochem. 75, 137–163.

Bungard, D., Fuerth, B.J., Zeng, P.Y., Faubert, B., Maas, N.L., Viollet, B., Carling, D., Thompson, C.B., Jones, R.G., and Berger, S.L. (2010). Signaling kinase AMPK activates stress-promoted transcription via histone H2B phosphorylation. Science 329, 1201–1205.

Buzzai, M., Jones, R.G., Amaravadi, R.K., Lum, J.J., DeBerardinis, R.J., Zhao, F., Viollet, B., and Thompson, C.B. (2007). Systemic treatment with the antidiabetic drug metformin selectively impairs p53-deficient tumor cell growth. Cancer Res. 67, 6745–6752.

Choo, A.Y., Yoon, S.O., Kim, S.G., Roux, P.P., and Blenis, J. (2008). Rapamycin differentially inhibits S6Ks and 4E-BP1 to mediate cell-type-specific repression of mRNA translation. Proc. Natl. Acad. Sci. USA 105, 17414–17419.

Davies, S.P., Sim, A.T., and Hardie, D.G. (1990). Location and function of three sites phosphorylated on rat acetyl-CoA carboxylase by the AMP-activated protein kinase. Eur. J. Biochem. 187, 183–190.

DeBerardinis, R.J., Lum, J.J., Hatzivassiliou, G., and Thompson, C.B. (2008). The biology of cancer: metabolic reprogramming fuels cell growth and proliferation. Cell Metab. 7, 11–20.

Düvel, K., Yecies, J.L., Menon, S., Raman, P., Lipovsky, A.I., Souza, A.L., Triantafellow, E., Ma, Q., Gorski, R., Cleaver, S., et al. (2010). Activation of a metabolic gene regulatory network downstream of mTOR complex 1. Mol. Cell 39, 171–183.

Egan, D.F., Shackelford, D.B., Mihaylova, M.M., Gelino, S., Kohnz, R.A., Mair, W., Vasquez, D.S., Joshi, A., Gwinn, D.M., Taylor, R., et al. (2011). Phosphorylation of ULK1 (hATG1) by AMP-activated protein kinase connects energy sensing to mitophagy. Science 331, 456–461.

Evans, J.M., Donnelly, L.A., Emslie-Smith, A.M., Alessi, D.R., and Morris, A.D. (2005). Metformin and reduced risk of cancer in diabetic patients. BMJ 330, 1304–1305.

Giardiello, F.M., Welsh, S.B., Hamilton, S.R., Offerhaus, G.J., Gittelsohn, A.M., Booker, S.V., Krush, A.J., Yardley, J.H., and Luk, G.D. (1987). Increased risk of cancer in the Peutz-Jeghers syndrome. N. Engl. J. Med. 316, 1511–1514.

Godlewski, J., Nowicki, M.O., Bronisz, A., Nuovo, G., Palatini, J., De Lay, M., Van Brocklyn, J., Ostrowski, M.C., Chiocca, E.A., and Lawler, S.E. (2010). MicroRNA-451 regulates LKB1/AMPK signaling and allows adaptation to metabolic stress in glioma cells. Mol. Cell 37, 620–632.

Gwinn, D.M., Shackelford, D.B., Egan, D.F., Mihaylova, M.M., Mery, A., Vasquez, D.S., Turk, B.E., and Shaw, R.J. (2008). AMPK phosphorylation of raptor mediates a metabolic checkpoint. Mol. Cell 30, 214–226.

Hadad, S.M., Baker, L., Quinlan, P.R., Robertson, K.E., Bray, S.E., Thomson, G., Kellock, D., Jordan, L.B., Purdie, C.A., Hardie, D.G., et al. (2009). Histological evaluation of AMPK signalling in primary breast cancer. BMC Cancer 9, 307.

Hallstrom, T.C., Mori, S., and Nevins, J.R. (2008). An E2F1-dependent gene expression program that determines the balance between proliferation and cell death. Cancer Cell 13, 11–22.

Hardie, D.G. (2011). AMP-activated protein kinase: an energy sensor that regulates all aspects of cell function. Genes Dev. 25, 1895–1908.

Hardie, D.G., Ross, F.A., and Hawley, S.A. (2012). AMPK: a nutrient and energy sensor that maintains energy homeostasis. Nat. Rev. Mol. Cell Biol. 13, 251–262.

Hatzivassiliou, G., Zhao, F., Bauer, D.E., Andreadis, C., Shaw, A.N., Dhanak, D., Hingorani, S.R., Tuveson, D.A., and Thompson, C.B. (2005). ATP citrate lyase inhibition can suppress tumor cell growth. Cancer Cell 8, 311–321.

Hawley, S.A., Boudeau, J., Reid, J.L., Mustard, K.J., Udd, L., Mäkelä, T.P., Alessi, D.R., and Hardie, D.G. (2003). Complexes between the LKB1 tumor suppressor, STRAD alpha/beta and MO25 alpha/beta are upstream kinases in the AMP-activated protein kinase cascade. J. Biol. 2, 28.

Hearle, N., Schumacher, V., Menko, F.H., Olschwang, S., Boardman, L.A., Gille, J.J., Keller, J.J., Westerman, A.M., Scott, R.J., Lim, W., et al. (2006). Frequency and spectrum of cancers in the Peutz-Jeghers syndrome. Clin. Cancer Res. 12, 3209–3215.

Huang, X., Wullschleger, S., Shpiro, N., McGuire, V.A., Sakamoto, K., Woods, Y.L., McBurnie, W., Fleming, S., and Alessi, D.R. (2008). Important role of the LKB1-AMPK pathway in suppressing tumorigenesis in PTEN-deficient mice. Biochem. J. 412, 211–221.

Imamura, K., Ogura, T., Kishimoto, A., Kaminishi, M., and Esumi, H. (2001). Cell cycle regulation via p53 phosphorylation by a 5′-AMP activated protein kinase activator, 5-aminoimidazole- 4-carboxamide-1-beta-D-ribofuranoside, in a human hepatocellular carcinoma cell line. Biochem. Biophys. Res. Commun. 287, 562–567.

Inoki, K., Zhu, T., and Guan, K.L. (2003). TSC2 mediates cellular energy response to control cell growth and survival. Cell 115, 577–590.

Jeon, S.M., Chandel, N.S., and Hay, N. (2012). AMPK regulates NADPH homeostasis to promote tumour cell survival during energy stress. Nature 485, 661–665.

Jones, R.G., and Thompson, C.B. (2009). Tumor suppressors and cell metabolism: a recipe for cancer growth. Genes Dev. 23, 537–548.

Jones, R.G., Plas, D.R., Kubek, S., Buzzai, M., Mu, J., Xu, Y., Birnbaum, M.J., and Thompson, C.B. (2005). AMP-activated protein kinase induces a p53-dependent metabolic checkpoint. Mol. Cell *18*, 283–293.

Jørgensen, S.B., Viollet, B., Andreelli, F., Frøsig, C., Birk, J.B., Schjerling, P., Vaulont, S., Richter, E.A., and Wojtaszewski, J.F. (2004). Knockout of the alpha2 but not alpha1 5′-AMP-activated protein kinase isoform abolishes 5-aminoimidazole-4-carboxamide-1-beta-4-ribofuranosidebut not contraction-induced glucose uptake in skeletal muscle. J. Biol. Chem. *279*, 1070–1079.

Keith, B., Johnson, R.S., and Simon, M.C. (2012). HIF1α and HIF2α: sibling rivalry in hypoxic tumour growth and progression. Nat. Rev. Cancer *12*, 9–22.

Kim, J.W., Tchernyshyov, I., Semenza, G.L., and Dang, C.V. (2006). HIF-1-mediated expression of pyruvate dehydrogenase kinase: a metabolic switch required for cellular adaptation to hypoxia. Cell Metab. *3*, 177–185.

Kim, J., Kundu, M., Viollet, B., and Guan, K.L. (2011). AMPK and mTOR regulate autophagy through direct phosphorylation of Ulk1. Nat. Cell Biol. *13*, 132–141.

Kim, Y.H., Liang, H., Liu, X., Lee, J.S., Cho, J.Y., Cheong, J.H., Kim, H., Li, M., Downey, T., Dyer, M.D., et al. (2012). AMPKα modulation in cancer progression: multilayer integrative analysis of the whole transcriptome in Asian gastric cancer. Cancer Res. *72*, 2512–2521.

Laplante, M., and Sabatini, D.M. (2009). mTOR signaling at a glance. J. Cell Sci. *122*, 3589–3594.

Levine, A.J., and Puzio-Kuter, A.M. (2010). The control of the metabolic switch in cancers by oncogenes and tumor suppressor genes. Science *330*, 1340–1344.

Li, Y., Xu, S., Mihaylova, M.M., Zheng, B., Hou, X., Jiang, B., Park, O., Luo, Z., Lefai, E., Shyy, J.Y., et al. (2011). AMPK phosphorylates and inhibits SREBP activity to attenuate hepatic steatosis and atherosclerosis in diet-induced insulin-resistant mice. Cell Metab. *13*, 376–388.

Liu, L., Cash, T.P., Jones, R.G., Keith, B., Thompson, C.B., and Simon, M.C. (2006). Hypoxia-induced energy stress regulates mRNA translation and cell growth. Mol. Cell *21*, 521–531.

Liu, L., Ulbrich, J., Müller, J., Wüstefeld, T., Aeberhard, L., Kress, T.R., Muthalagu, N., Rycak, L., Rudalska, R., Moll, R., et al. (2012). Deregulated MYC expression induces dependence upon AMPK-related kinase 5. Nature *483*, 608–612.

Lum, J.J., Bui, T., Gruber, M., Gordan, J.D., DeBerardinis, R.J., Covello, K.L., Simon, M.C., and Thompson, C.B. (2007). The transcription factor HIF-1alpha plays a critical role in the growth factor-dependent regulation of both aerobic and anaerobic glycolysis. Genes Dev. *21*, 1037–1049.

MacIver, N.J., Blagih, J., Saucillo, D.C., Tonelli, L., Griss, T., Rathmell, J.C., and Jones, R.G. (2011). The liver kinase B1 is a central regulator of T cell development, activation, and metabolism. J. Immunol. *187*, 4187–4198.

Mayer, A., Denanglaire, S., Viollet, B., Leo, O., and Andris, F. (2008). AMP-activated protein kinase regulates lymphocyte responses to metabolic stress but is largely dispensable for immune cell development and function. Eur. J. Immunol. *38*, 948–956.

Mullen, A.R., Wheaton, W.W., Jin, E.S., Chen, P.H., Sullivan, L.B., Cheng, T., Yang, Y., Linehan, W.M., Chandel, N.S., and DeBerardinis, R.J. (2012). Reductive carboxylation supports growth in tumour cells with defective mitochondria. Nature *481*, 385–388.

Papandreou, I., Cairns, R.A., Fontana, L., Lim, A.L., and Denko, N.C. (2006). HIF-1 mediates adaptation to hypoxia by actively downregulating mitochondrial oxygen consumption. Cell Metab. *3*, 187–197.

Robert, F., Carrier, M., Rawe, S., Chen, S., Lowe, S., and Pelletier, J. (2009). Altering chemosensitivity by modulating translation elongation. PLoS ONE *4*, e5428.

Semenza, G.L. (2011). Oxygen sensing, homeostasis, and disease. N. Engl. J. Med. *365*, 537–547.

Shackelford, D.B., and Shaw, R.J. (2009). The LKB1-AMPK pathway: metabolism and growth control in tumour suppression. Nat. Rev. Cancer *9*, 563–575.

Shackelford, D.B., Vasquez, D.S., Corbeil, J., Wu, S., Leblanc, M., Wu, C.L., Vera, D.R., and Shaw, R.J. (2009). mTOR and HIF-1alpha-mediated tumor metabolism in an LKB1 mouse model of Peutz-Jeghers syndrome. Proc. Natl. Acad. Sci. USA *106*, 11137–11142.

Shaw, R.J., Bardeesy, N., Manning, B.D., Lopez, L., Kosmatka, M., DePinho, R.A., and Cantley, L.C. (2004a). The LKB1 tumor suppressor negatively regulates mTOR signaling. Cancer Cell *6*, 91–99.

Shaw, R.J., Kosmatka, M., Bardeesy, N., Hurley, R.L., Witters, L.A., DePinho, R.A., and Cantley, L.C. (2004b). The tumor suppressor LKB1 kinase directly activates AMP-activated kinase and regulates apoptosis in response to energy stress. Proc. Natl. Acad. Sci. USA *101*, 3329–3335.

Svensson, R.U., and Shaw, R.J. (2012). Cancer metabolism: Tumour friend or foe. Nature *485*, 590–591.

Vander Heiden, M.G., Cantley, L.C., and Thompson, C.B. (2009). Understanding the Warburg effect: the metabolic requirements of cell proliferation. Science *324*, 1029–1033.

Wu, M., Neilson, A., Swift, A.L., Moran, R., Tamagnine, J., Parslow, D., Armistead, S., Lemire, K., Orrell, J., Teich, J., et al. (2007). Multiparameter metabolic analysis reveals a close link between attenuated mitochondrial bioenergetic function and enhanced glycolysis dependency in human tumor cells. Am. J. Physiol. Cell Physiol. *292*, C125–C136.

Xu, Q., Vu, H., Liu, L., Wang, T.C., and Schaefer, W.H. (2011). Metabolic profiles show specific mitochondrial toxicities in vitro in myotube cells. J. Biomol. NMR *49*, 207–219.

Zheng, B., Jeong, J.H., Asara, J.M., Yuan, Y.Y., Granter, S.R., Chin, L., and Cantley, L.C. (2009). Oncogenic B-RAF negatively regulates the tumor suppressor LKB1 to promote melanoma cell proliferation. Mol. Cell *33*, 237–247.

Zhou, G., Myers, R., Li, Y., Chen, Y., Shen, X., Fenyk-Melody, J., Wu, M., Ventre, J., Doebber, T., Fujii, N., et al. (2001). Role of AMP-activated protein kinase in mechanism of metformin action. J. Clin. Invest. *108*, 1167–1174.